Proceedings of the ASME 2010 3rd Joint US-European Fluids Engineering Summer Meeting and 8th International Conference on Nanochannels, Microchannels, and Minichannels
FEDSM-ICNMM2010
August 1-5, 2010, Montreal, Canada

FEDSM-ICNMM2010-30022

SENSITIVITY OF THE PREDICTIVE STRUCTURAL MODELS UNDER STOCHASTIC AND CONVECTIVE EXCITATION

F. Franco*, S. De Rosa
Department of Aerospace Engineering
Università di Napoli "Federico II", Napoli, Italy
Email: francof@unina.it; derosa@unina.it

E. Ciappi, F. Magionesi
INSEAN
Via di Vallerano, Roma, Italy
Email: e.ciappi@insean.it; f.magionesi@insean.it

ABSTRACT
The quality of the predictive response of a structural domain, under a random and convective load, is here analyzed by discussing each step of the numerical procedure. The structural response, due to a wall pressure distribution, is derived in modal coordinates according to a finite element scheme. The modal basis can include the dry or wet (aeroelastic) structural mode shapes: in the present analysis only the in vacuum eigenvectors are used.
For such a problem one of the most critical points is the transformation of the pressure distribution into discrete locations. In fact, this step depends on (i) the assumed TBL model, (ii) the integration scheme and (iii) the frequency range. These three points are the goals of the present work where the specific sensitivity to each of them is investigated. The transformation of the pressure distribution into discrete locations can be computationally expensive for the desired level of the required numerical approximation. The use of consistent formulation in the finite element scheme can be unfeasible. Moreover the approximations, in expressing the pressure field, can have a different influence on the structural responses according to the chosen TBL models. This is another key aspect of the present work.

INTRODUCTION
The turbulent boundary layer (TBL) is one of the most important sources of vibration and noise in automotive, aerospace, and railway transportation. The stochastic pressure distribution associated with the turbulence is able to excite significantly the structural response and the related acoustic radiated power. The problem is intrinsically multidisciplinary since it involves the mechanical vibrations, the aerodynamics, and the external/internal acoustics.

The spatial characterisation of wall pressure fluctuations (WPFs) was first analyzed by Corcos [1] on the basis of measurements performed by Willmarth and Wooldridge [2]. Assuming the validity of the separation of variables in streamwise and spanwise directions, Corcos stated an exponential decay for the cross spectral density (CSD) as a function of the similarity variables $\omega\xi/U_c$ and $\omega\eta/U_c$ where U_c is the convection velocity, ω is the circular frequency and ξ, η are the streamwise and spanwise spatial separations, respectively.

Several authors have performed comparisons between measured CSD data and the Corcos model [3-5]. At least these analyses, in a certain non-dimensional frequency range, confirmed the hypothesized pressure behaviour for a wide series of spatial separations in streamwise direction and for different flow velocities or local Reynolds number values. Notwithstanding, it is generally stated that the Corcos model gives a correct representation of the WPF behaviour in the convective domain *i.e.* when the structural wavenumbers are close to the convective one $k_c=\omega/U_c$. On the contrary, in the subconvective domain, the white Corcos spectrum largely overpredicts the real amplitude. Several new models, some directly derived from the Corcos one [6-7], others overcoming the Corcos multiplicative approach [8-9] were developed to improve the estimation of pressure spectra.

The prediction of the structural response and of the radiated acoustic power has an intrinsic complexity too. The predictive methodologies can be roughly grouped in two different families. The first is represented by the modal methods in which commonly all the required operators are expanded by using the structural in vacuum undamped mode shapes and natural frequencies. Improvements can be performed by accounting also the aeroelastic interaction and/or by using

* Address all correspondence to this author.

complex modal basis. The energy methods constitute the second group: the target is to obtain a spatially-averaged representation of the structural (and acoustic) response. For increasing values of the modal overlap factor (the product among excitation frequency, modal density and damping), the efficiency and the efficacy of the energy methods become undoubted: they are able to give the global response with the lowest computational costs. At the same time, when the value of the modal overlap factor is less than unit value, the response is still dominated by the well resonating modes and therefore, the modal methods are still useful since they furnish a solution with local characteristics. Which methodology is the better for closing the gap from low to high values of the modal overlap factors is still an open question.

Both solution families have to face the difficulties associated to the real structural configurations (i.e. plates with full set of stringers, frame, etc. or with new orthotropic materials as composite ones). For these reasons there is still a scientific interest in developing innovative and fast solutions (i.e. computationally cheap) for the stochastic response of a plate [10-18]. Most of these works addressed the problem of the applicability of the deterministic simulations (finite elements and spectral finite elements) under wall pressure fluctuation load.

The most critical point is the transformation of the pressure distribution into discrete locations. In fact, this step depends on (i) the assumed TBL model, and (ii) the integration scheme and (iii) the frequency range. Each choice has an direct effect on the predicted structural response. The present work analyzes these aspects with reference to the sensitivity and accuracy on the structural response. Moreover, it investigates the possibility to reduce the computational cost keeping the same level of accuracy.

NOMENCLATURE

a	stream-wise plate length
A_{QjQk}	joint acceptance between the *j*th and *k*th modes
Area	plate area
b	cross-wise plate length
E	Young's modulus
h	plate thickness
H_i	*i*th term of the diagonal structural transfer functions matrix for the plate in finite element approach $[NM * NM]$
i	imaginary unit
k_c	convective wavenumber
NG	number of solution points for the evaluation of the mean response or number of grid of the finite element mesh
NM	number of retained structural eigensolutions for evaluating the response
R	non-dimensional metric response
$\mathbf{S_{FF}}$	load matrix in finite element approach $[NG * NG]$
S_p	auto spectral density of the wall pressure distribution due to the turbulent boundary layer
S_w	auto spectral density of the plate displacement
$\overline{S}_W$	mean auto spectral density of the plate displacement
$\mathbf{S_\Phi}$	modal random load matrix in finite element approach $[NM * NM]$
U_∞	free stream (undisturbed) speed
U_C	convective speed ($U_C = \beta_C U_\infty$)
w	out-of-plane displacement of the plate
x	stream-wise reference axis
X_{pp}	cross spectral density of the wall pressure distribution due to the turbulent boundary layer
$\mathrm{X_w}$	cross spectral density matrix of the plate displacement
y	cross-wise reference axis
Z_j	plate dynamic impedance for the *i*th mode

Greek Symbols

α_x	stream wise correlation coefficient
α_y	cross stream wise correlation coefficient
β_C	convective constant
γ_j	generalised mass coefficient for the plate *j*th mode
Γ	coherence function
Δx	extension of each finite element in stream wise direction
Δy	extension of each finite element in cross stream wise direction
η	structural damping factor
ξ_x	stream-wise separation distance
ξ_y	cross-wise separation distance
ρ	material density
ψ_i	*i*th analytical mode shape of the plate, *i*th column vector belonging to $\mathbf{\Phi}$

$\mathbf{\Phi}$	matrix of the modal shape in finite element modal approach [$NG * NM$]
ω	circular excitation frequency
ω_j	natural circular frequency of the jth mode

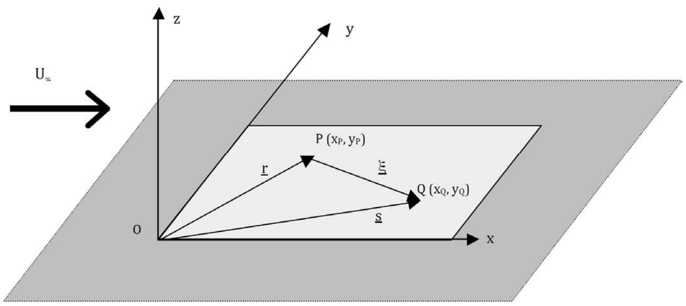

FIGURE 1: THE ELASTIC PLATE.

THE REFERENCE MODELS

The Corcos Model

The model formulated by Corcos [1], on the basis of experimental evidence of some properties of the fluctuating pressure field, expressed the cross spectral density as a product of functions in longitudinal and lateral direction separately:

$$X_{pp}(\xi,\omega) = S_p(\omega)\Gamma(\xi,\omega)\,; \tag{1}$$

$$X_{pp}\left(\xi_x,\xi_y,\omega\right) = S_p(\omega)\,\mathrm{e}^{-\alpha_x\left|\frac{\omega\xi_x}{U_c}\right|}\,\mathrm{e}^{-\alpha_y\left|\frac{\omega\xi_y}{U_c}\right|}\,\mathrm{e}^{-\frac{\mathrm{i}\omega\xi_x}{U_c}}\,. \tag{2}$$

The Corcos model, here briefly recalled, is among the simplest representations of the wall pressure distribution due to a turbulent boundary layer, since (i) the space variables are separated, (ii) the phase variation is only accounted along the stream-wise direction, (iii) all functions have the same exponential form, and (iv) it is independent from any couple of points and depends only on their distance.

The Corcos model is an empirical model and the coefficients α_x and α_y are determined from measurements of the spatial coherence between two points of the wall pressure fluctuations. Other models have been proposed in literature overcoming some limitations of the Corcos model [6,8-9]. Moreover the Corcos model has a strong predictive character since the empirical coefficients, appearing in its expression, can be considered universal for fully developed TBL in zero pressure gradient flow. Finally, it allows closed form expression for the response of simple structures such as simply supported flat plates.

In the present paper both analytical and numerical structural responses are derived according to the Corcos model. It is well known that this TBL model does not fit correctly the experimental data as frequency increases. The limitation of the Corcos model lies in its convective character in fact, it works well in the convective domain *i.e.* below the aerodynamic coincidence frequency. Nevertheless, as already stated above, it allows closed-form expressions and, therefore, it is useful for the sensitivity analyses of the present work. Moreover, its mathematical simplicity justifies the use of the Corcos model even in wide frequency ranges, as done recently in the scientific literature too, [16, 18].

Hence, the use of the Corcos model does not affect the sensitivity analyses which are the objectives of the present work. In fact, the numerical results can be discussed in a relative manner.

The Plate Response

The plate is thin, flat, rectangular and isotropic with no pre-stress (no pressurisation and no edge loadings). The plate is simply supported on all four edges. It is mounted in an infinite rigid plane baffle flush with the TBL, Fig.1. The plate lies in an *xy* plane, and the flexural out-of-plane displacements, named $w(x,y,t)$, are along the z axis. The flow is along the x axis. The plate characteristics are in Tab.1.

TABLE 1: THE PLATE CHARACTERISTICS.

Symbol	Value	Description
a	0.768 m	stream wise side
b	0.328 m	cross stream wise side
h	0.0016 m	Thickness
E	7.0 10^{10} Pa	elasticity modulus
ρ	2700 kg m^{-3}	mass density

In the present analysis it is assumed that any fluid-loading effect on the structural dynamic response can be neglected. The displacement cross spectral density between any arbitrary couple of points belonging to a thin, isotropic and homogeneous plate, $A(x_A,y_A)$ and $B(x_B,y_B)$, due to an assigned stochastic distributed excitation, can be found with the following modal expansion, as given in [19]:

$$X_w\left(x_A,y_A,x_B,y_B,\omega\right) = \sum_{j=1}^{\infty}\sum_{n=1}^{\infty}\left[\frac{\psi_j\left(x_A,y_A\right)\psi_n\left(x_B,y_B\right)}{Z_j^*(\omega)Z_n(\omega)}\right]\left[\frac{S_p(\omega)(ab)^2}{\gamma_j\gamma_n}\right]A_{Q_jQ_n}(\omega) \tag{3}$$

with

$$A_{Q_jQ_n}(\omega)=\int_0^a\int_0^a\int_0^b\int_0^b\left[\frac{X_{pp}(x,y,x',y',\omega)}{S_p(\omega)(ab)^2}\psi_j(x,y)\psi_n(x',y')\right]\mathrm{d}y\mathrm{d}y'\mathrm{d}x\mathrm{d}x' \quad (4)$$

and

$$\gamma_j=\int_0^a\int_0^b\psi_j^2(x,y)\mathrm{d}y\mathrm{d}x;\quad Z_j(\omega)=\rho h\left[\omega_j^2-\omega^2+\mathrm{i}\eta\omega_j^2\right]. \quad (5)$$

The integrals defined by the symbol A_{QjQk} are well known also as the acceptances: joint acceptance for $j=k$, or cross acceptance for $j\neq k$. Further, the formulation contained in the Eqs.(3) and (4) can be applied to any structural operator once its modal basis is known. In particular, in the above equations, a hysteretic model for the structural damping is assumed.

The auto spectral density of the displacement at a selected point is given as follows:

$$S_w(x_A,y_A,\omega)=\sum_{j=1}^{\infty}\sum_{n=1}^{\infty}\left[\frac{\psi_j(x_A,y_A)\psi_n(x_A,y_A)}{Z_j^*(\omega)Z_n(\omega)}\right]\left[\frac{S_p(\omega)}{\gamma_j\gamma_n}\right](ab)^2A_{Q_jQ_n}(\omega). \quad (6)$$

It has to be noted that this last quantity is strictly real. It should also be noted that it is possible to evaluate the plate mean response by using the following relationship:

$$\bar{S}_W(\omega)=\frac{1}{\text{Area}}\int_{\text{Area}}S_w(x,y,\omega)\mathrm{d}x\mathrm{d}y\,. \quad (7)$$

In the above modal expansions, Eqs. (3) and (6), the proper number of the total modal components, *NM*, have to be selected in order to achieve convergence of the results for the assigned excitation frequency.

For sake of brevity, the analytical derivations of Eqs. (3-6) are not reported in the present work. All details can be found in [19].

Assuming a simply supported plate and a Corcos model for the WPFs, the integrals in Eqs. (4) and (5) have a closed-form analytical solution. Hence, in the present work, all results named as “analytical” are carried out with Eqs. (6) and (7). The analytical results represent a reference solution for the numerical analyses.

The numerical results are developed through a scheme in discrete coordinates. A standard finite element procedure can be assembled by using the following equation suitable for all the methods working with discrete coordinates [19]. The cross spectral density matrix of displacements of a structural operator, represented by using *NG* degrees of freedom and *NM* mode shapes, is given by:

$$\mathbf{S_W}(\omega)=\mathbf{\Phi}\,\mathbf{H}(\omega)\mathbf{S_\Phi}(\omega)\mathbf{H}(\omega)^*\,\mathbf{\Phi}^{\mathrm{T}} \quad (8)$$

with

$$H_j(\omega)=\left[\omega_j^2-\omega^2+\mathrm{i}\eta\omega_j^2\right]^{-1}$$
$$\mathbf{S_\Phi}(\omega)=\mathbf{\Phi}^{\mathrm{T}}\,\mathbf{S_{FF}}(\omega)\mathbf{\Phi}\,. \quad (9)$$

The matrix $\mathbf{S_W}$, in Eq. (8), allows the derivation of the mean spectral density of the plate displacement, as introduced in Eq. (7), through the average of its diagonal terms. The orthogonality property of the modal bases strongly reduces the computational cost associated with the evaluation of the mean spectral density of the plate displacement.

All results herein named as “numerical” are carried out with Eqs. (8) and (9). The presented numerical results differ in the numerical representation of the $\mathbf{S_{FF}}$ matrix and in the assumed modal bases.

The main problem of any approach using discrete coordinates is the translation of the distributed random loads to the set of *NG* points, in other words the way of representing the $\mathbf{S_{FF}}$ matrix. A simplified approach refers to each grid point rather than each finite element. This means that the load acting on the *i*th grid point will be the resultant of the distributed load working on the equivalent nodal area belonging to it. This area vector can be evaluated easily by using a static deterministic unit pressure load [13, 20]. Accordingly, one gets the generic *ij*th member of the $NG\times NG$ $\mathbf{S_{FF}}$ matrix:

$$SC_{FF\;i,j}^{(G)}=\int_{x_i-\frac{\Delta x}{2}}^{x_i+\frac{\Delta x}{2}}\int_{x_j-\frac{\Delta x}{2}}^{x_j+\frac{\Delta x}{2}}\int_{y_i-\frac{\Delta y}{2}}^{y_i+\frac{\Delta y}{2}}\int_{y_j-\frac{\Delta y}{2}}^{y_j+\frac{\Delta y}{2}}X_{pp}(x_i,x_j,y_i,y_j,\omega)\mathrm{d}y_j\mathrm{d}y_i\mathrm{d}x_j\mathrm{d}x_i\,. \quad (10)$$

An area $\Delta x\cdot\Delta y$ is assigned to both the points $P(x_i,y_i)$ and $Q(x_j,y_j)$ and the double space integration refers to these finite domains.
A further approximation could also be introduced considering that the wall pressure distribution due to the TBL in the low frequency ranges does not fluctuate very quickly in a small area $\Delta x\cdot\Delta y$. In this case the last integral could be approximated as follows:

$$SL_{FF\;i,j}^{(G)}=X_{pp}(x_i,x_j,y_i,y_j,\omega)[\Delta x\Delta y]^2\,. \quad (11)$$

The approximation in Eq. (11) is more and more acceptable as the area $\Delta x\cdot\Delta y$ decreases. The differences, introduced by the approximations in representing the $\mathbf{S_{FF}}$ matrix, Eqs.(10) and (11), are discussed in the next Sections. This analysis is done keeping always constant the discretization area $\Delta x\cdot\Delta y$ between the two possible approximations in Eqs. (10) and (11).

Figure 2 shows the complexity to translate a convective aerodynamic load in a discrete coordinate field as also stated recently for a one-dimensional domain, [18].

In the present work the numerical results are carried out for two values of the asymptotic flow speed: 100 m/s and 50 m/s. The structural mesh is designed to reproduce the flexural wavelength up to 8.0 kHz (4343 grids: 101 along the *x* axis and 43 along the *y* axis; 380 eigenvectors). The finite element scheme uses plate elements with four nodes. Eigenvectors and eigenvalues are carried out with the real modal analysis algorithm of the MSC/NASTRAN solver (Lanczos Method).

The convective coincidence frequencies are respectively 537 Hz and 110 Hz. Hence, Figure 2 shows that according to this mesh size the convective load is correctly represented up to 1500 Hz and less than 1000 Hz respectively for 100 m/s and 50 m/s.

Any numerical procedure is more and more approximated as frequency increases above the coincidence frequency due to the load representation. The accuracy of the the transformation of the pressure distribution into discrete locations, at increasing frequency, does not depend on the particular TBL model.

In general, in structural dynamics and interior/exterior noise problems, the frequency range of interest is up the audible ones and the high frequency range is identified through the value of the modal overlap factor. When the load has convective characteristics the high frequency range is ruled by the coincidence frequency, too. In the present work, for the assumed value of the structural damping, the modal overlap function reaches the unit value around 700 Hz and the coincidence frequencies are 537 Hz and 110 Hz respectively for 100 m/s and 50 m/s.

THE NUMERICAL RESULTS

The Metric

The numerical results are carried out with the following set of parameters: α_x=0.116; α_y=0.700; β_c=0.8.

The structural damping of the plate, η, is assumed constant: η=0.02.

A nondimensional metric for the response of the plate is defined through the quantity R:

$$R(\omega) = \frac{\omega^4 (\rho h)^2 \overline{S}_W(\omega)}{S_p(\omega)}. \tag{12}$$

This metric is used to discuss the results of the present work. In this way the structural response does not depend on the power spectral density of the wall pressure fluctuations which is only a multiplicative factor. The numerator is a measure of the vibration energy of the plate.

Approximations in the Load Discretization

In ref. [15] it is presented a comparison between the numerical results and the analytical one for the same test-article of the present work. In ref. [15] the numerical procedure is based on the same Eqs. (8) and (9) and those results were derived with a former modal basis which led to rounding problems in the numerical procedure. A better numerical treatment of the eigenvectors allows the development of an enhanced result. It has to be underlined that above 500 Hz, for a flow speed equal to 100 m/s, the translation of the load matrix becomes frequency by frequency more complex according to wavelength evolution, as in Fig. 2.

A new comparison of the numerical results is shown in Fig. 3. Both numerical results in Fig. 3 are carried out according to the load approximation in Eq. (11).

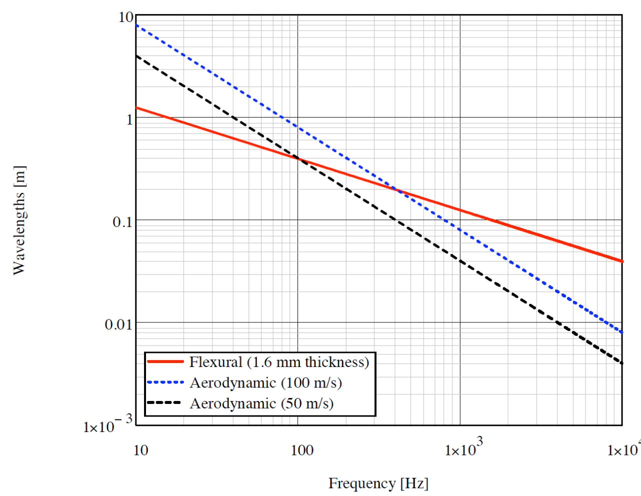

FIGURE 2: THE FLEXURAL AND AERODYNAMIC WAVELENGHTS VS. FREQUENCY.

With a good-conditioned modal basis the FEM based numerical solution is able to follow the analytical one in a larger frequency band. Nevertheless, the translation of the TBL load over a discrete structural mesh leads in any case to the divergence of the numerical curve from the analytical one. This effect is more and more evident for a lower flow speed, Fig. 4.

This divergence is in agreement with the analysis of the structural and aerodynamic wavelengths and with the approximation introduced by the Eq. (11).

The Corcos TBL model and the use of a uniform structural mesh, with rectangular finite element domains, allow an analytical expression of the Eq. (10). Then, it is possible to evaluate the benefits in using a different approximation in the expression of the elements of the $\mathbf{S_{FF}}$ matrix. This comparison is reported in Figs. 5 and 6.

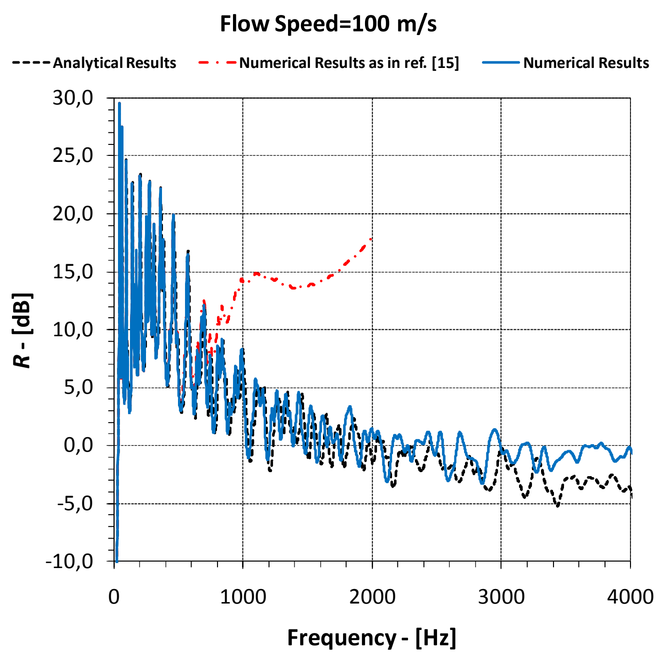

FIGURE 3: COMPARISON AMONG ANALYTICAL AND NUMERICAL RESULTS WITH DIFFERENT APPROXIMATIONS IN THE MODAL BASES.

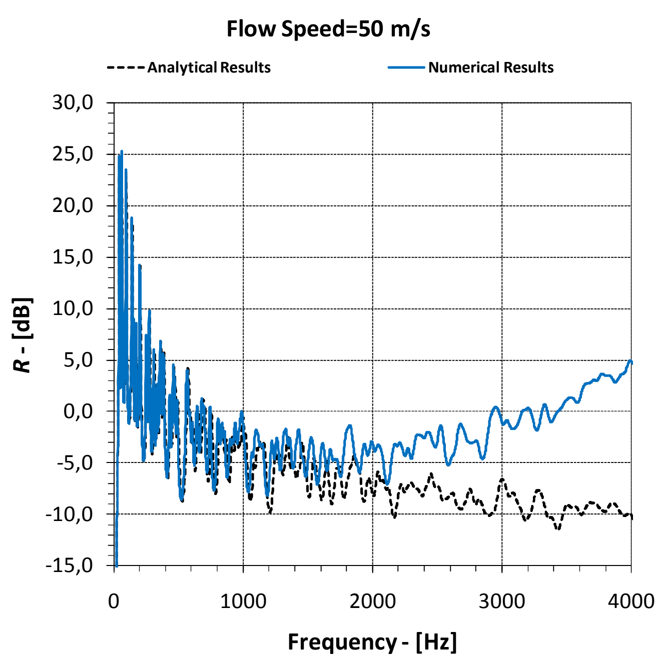

FIGURE 4: COMPARISON AMONG ANALYTICAL AND NUMERICAL RESULTS – EFFECT OF THE LOAD DISCRETIZATION.

The load discretization, according to Eq. (10), leads to a significant improvement of the numerical results. Nevertheless for the asymptotic flow speed equal to 50 m/s, or lower, the structural response diverges again at a frequency lower than the design frequency of the structural mesh, (see Fig. 6 above 4kHz).

Moreover, the analytical derivation of the the $\mathbf{S_{FF}}$ matrix elements, as in Eq.(10), is feasible only if the TBL model can be easily integrated and the integration domain (structural element domain) has a regular geometry. If both conditions are satisfied the numerical procedure does not require an additional computational cost because the assembly of the $\mathbf{S_{FF}}$ matrix does not involve a numerical integration.

It is not worth noting that in general the computational cost to develop the structural response at high frequency is unacceptable and therefore some authors have proposed enhanced numerical methods, as for example in [15, 16, 18], to accomplish the high frequency bands. On the contrary, the load approximation of the $\mathbf{S_{FF}}$ matrix elements of Eq.(11) remains acceptable in the low frequency bands.

Most of the above mentioned enhanced numerical methods requires that the wall pressure fluctuations can be modeled as uncorrelated loadings and the structural domain presents a high modal overlap factor; i.e. they do not deal with the mid-frequency range. On the contrary, at decreasing flow speed, the frequency range of validity of Eq. (11) reduces strongly and the mid-frequency bands becomes more relevant in the structural response.

Simplified Numerical Models

The solution procedure outlined in Eqs. (8) and (9) has an increasing computational cost as frequency increases. In fact, the solution cost is clearly linked to the number of degrees of freedom and number of modal components (*NG* and *NM* respectively). As already stated, NG depends on the convective characteristics of the load, too. These computational aspects have more and more importance if the solution domain is not as simple as a flat panel (i.e. some structural bays of an aircraft or of a cruise ship).

A FEM scheme can deal with complex structural configurations taking into account the full set of structural details (composite materials, structural stiffeners, etc.). This flexibility in the solution is related to the use of the modal characteristics of the structural domain.

The derivation of the $\mathbf{S_{FF}}$ matrix elements, as in Eq. (11), allows the solution with any TBL model even if its function is not based on scheme with separable variables. Therefore, the computational cost of this approach is justified by the versatility in the choice of the TBL model.

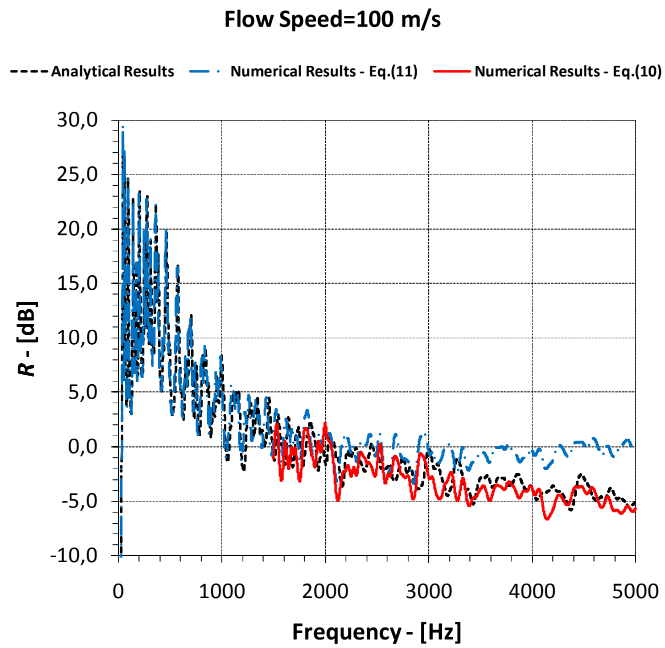

FIGURE 5: : COMPARISON AMONG ANALYTICAL AND NUMERICAL RESULTS – IMPROVEMENTS IN THE LOAD DISCRETIZATION.

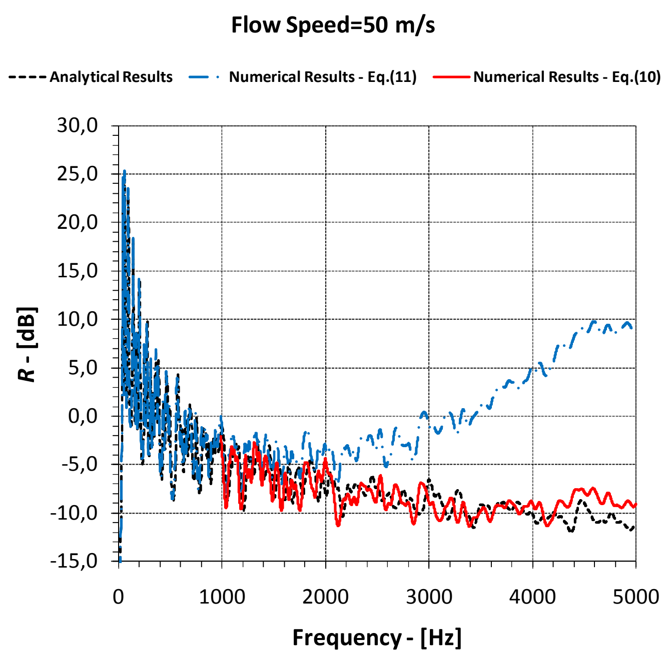

FIGURE 6: COMPARISON AMONG ANALYTICAL AND NUMERICAL RESULTS – IMPROVEMENTS IN THE LOAD DISCRETIZATION.

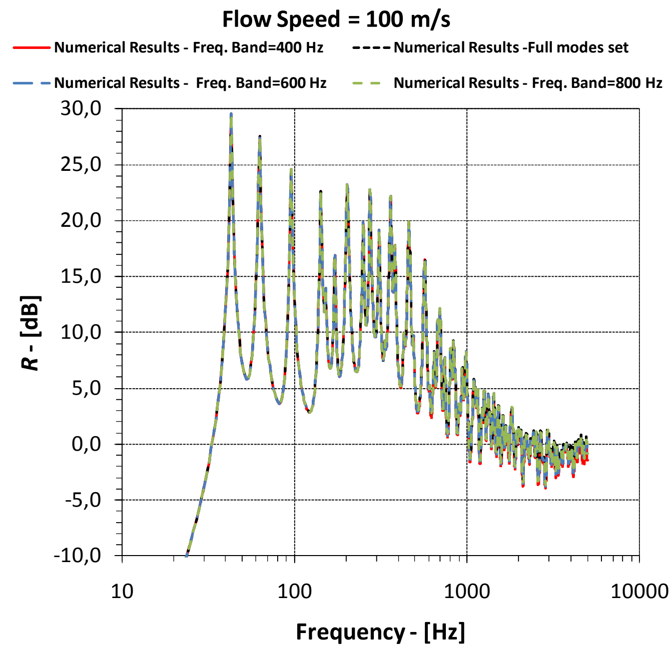

FIGURE 7: NUMERICAL RESULTS WITH DIFFERENT MODAL BASES.

In this section all numerical results are developed according to the Eq. (11). Figure 7 shows the convergence of the numerical solutions using a smaller modal basis. The different numerical solutions use, at each solution frequency, the number of eigenvectors resonating in an assigned frequency band. The number of eigenvectors for each solution is 10, 30 and 40 for the frequency bands of 400, 600 and 800 Hz respectively and the reduction of the computational cost for each solution frequency is 41%, 37% and 34%. There are few differences in the high frequency range but the four curves are almost coincident. The results for a flow speed equal to 50 m/s are analogous and they are not reported here for sake of brevity. Hence, it is unnecessary the use of the complete set of the modal bases. An iterative procedure can be programmed in order to use the minimum number of eigenvectors which guarantees the convergence of the numerical solution (i.e. any further modal component does not change the numerical result). It is also obvious that the minimum number of eigenvectors depends on the structural damping.

Another key aspect is the predictive capability of the solution scheme. The Corcos model (and in general the $\mathbf{S_{FF}}$ matrix) requires the knowledge of the aerodynamic characteristics of the flow. In particular, the derivation of the correlation coefficients needs expensive experimental measurements and their interpretation is often very complex. In general, the metric *R*, in Eq.(12), reduces the necessary data on the flow characteristics.

In addition, some simplified correlation functions can be analyzed. An incident diffuse field is represented by an infinite sum of uncorrelated plane waves [16]. The coherence function is given by

$$\Gamma(\xi_x, \xi_y, \omega) = \frac{\sin(\omega\xi_x/U_c)}{\omega\xi_x/U_c} \cdot \frac{\sin(\omega\xi_y/U_c)}{\omega\xi_y/U_c} \quad (13)$$

where only the convective constant is necessary. Figures 8 and 9 show the comparison among the different coherence functions for two flow speeds. It is evident that the low frequency region is well predicted by the assumption of incident diffuse field: it is the frequency range associated with the highest vibration energy and the best predictive capabilities of the Corcos model. The good prediction of the first structural resonances can lead also to a good estimation of the acoustic radiated power in the same frequency range. These results, obtained with a simplified model, have a quality lower than those obtainable with any complete TBL model. Nevertheless, the coherence model in Eq. (13) does not require any information on the wall pressure fluctuations only with the exception of the convective speed.

For increasing frequency the capability to translate the TBL load on the finite element mesh diminishes. But it is well-known that in the high frequency bands the TBL load is similar to a totally uncorrelated pressure field. The authors in ref. [18] have analyzed the structural response of a flexural beam (one dimensional domain) for increasing excitation frequency. For a one dimensional domain they proposed a compensation procedure to take into account the loss of the load correlation due to the coarse mesh. The compensation procedure was mathematically derived for the frequency range in which the TBL load can be considered totally uncorrelated. In the present work, the expression presented in [18], for a one-dimensional domain, is extended to a two-dimensional one without deriving it again with a rigorous mathematical analysis. If the TBL load can be considered totally uncorrelated the $\mathbf{S_{FF}}$ matrix is diagonal. The proposed expression is

$$S_{FF}^{i,i} = \frac{\alpha_x \cdot (1+\alpha_x^2)\delta_x}{\omega/U_c} \cdot \frac{\alpha_y \cdot (1+\alpha_y^2)\delta_y}{\omega/U_c} \quad (14)$$

where $\delta_x = \pi \cdot \Delta x,\ \delta_y = \pi \cdot \Delta y$. The Eq. (14) has been verified for two flow speeds and represents only a best fit of the analytical results. The numerical results are shown in Figs. 10 and 11 and are presented only in the high frequency range. The horizontal axis of these figures and of the next ones is in logarithmic scale and the vertical gridlines have a frequency step of 500 Hz.

The compensation procedure allows an acceptable prediction of the structural response in the high frequency bands with a very low computational cost due to diagonal form of the $\mathbf{S_{FF}}$ matrix. The compensation procedure extends the validity of the finite element mesh. As expected its accuracy is lower toward the low frequency band because the hypothesis of uncorrelated load for the WPFs is less valid.

Figures 10 and 11 show the results of another formulation too. This additional formulation uses the following expression for the $\mathbf{S_{FF}}$ matrix, [16], being again this diagonal:

$$S_{FF}^{i,i} = \frac{4\omega^2}{U_c^2} \cdot \frac{\alpha_x \cdot \Delta x \cdot \Delta y}{\alpha_y \cdot (1+\alpha_x^2)}. \quad (15)$$

The Eq. (15) is derived applying the spatial extent equivalence to a TBL excitation defined through a Corcos model, [16]. The spatial extent equivalence leads to a rain on the roof excitation that can reproduce a Corcos like TBL in the high frequency range.

Figures 10 and 11 allow a comparison of the load approximations in Eqs. (14) and (15). In general, over the whole frequency range, the approximation of Eq. (15) has a better accuracy but its accuracy decreases with increasing flow speed in the lower frequency bands.

The results of previous Eqs. (14) and (15) can be applied to those numerical methods that reduce the computational cost through the solution of a transformed solution domain, [15,21]. In particular, the approximation of Eq. (15) has been applied to a “scaled” plate in order to verify the accuracy of the results. The methodology to scale the structural domain is not reported here for sake of brevity, [15,21]. Basically the in-plane dimensions of the plate are scaled by a given factor and, at the same time, the structural damping is properly augmented. The relationship between the augmented structural damping and the scaling factor is ruled by a properly defined law according to the requested level of accuracy of the solution. Up to date, the scaling procedure allows only the prediction of the plate mean response.

This numerical procedure allows a drastic reduction on the number of the structural nodes and eigenvectors with a significant benefit in the overall computational cost. The results of the scaled model in Figs. 12 and 13 are derived with a 1122 grids and 94 eigenvectors. The accuracy of the results is in agreement with the approximation introduced with the Eq. (15) and the scaling procedure. In the frequency range with a low modal overlap factor, the lower accuracy of the predicted structural response, with a scaled model, is balanced by the advantages in terms of computational cost, as summarized in Tab.2:

TABLE 2: RELATIVE COMPUTATIONAL COST.

Approximation	Elapsed Time/Frequency Step	Cost Factor
Full Load Matrix	1.0	5000
Eq.(14) or Eq.(15)	5.0E-3	25
Scaled Model	2.0E-4	1

In many engineering problems the availability of key-design information, as the mean vibration energy level in a frequency band, can guide and rule the successive detailed design of a complex structural system. A fast computational procedure can be useful because computational iterations, with a higher accuracy, can be developed in a second phase of the design work.

CONCLUSIONS

The present paper discusses the numerical procedures to predict the structural vibrations under a turbulent boundary layer load. Different approximations of the TBL load matrix are presented and analyzed with reference to the accuracy of the predicted structural response. Some of the presented approximations reduce the amount of the necessary experimental data and/or the computational cost. These latter aspects are both key-elements in the analysis of the predictive capabilities of a numerical procedure for the evaluation of the structural response under a TBL excitation.

The present paper analyzes the numerical results using two values of the flow speed in order to outline the role of the convective load characteristics versus the structural ones.

The simplified load models, for the high frequency range, highlight the possibility to represent the TBL excitation with a reduced computational cost but keeping a high level of the accuracy in the predicted structural response.

The simplified load models, for the high frequency range, are derived according to the Corcos model for the TBL. It is well known that the Corcos model is mathematically simple and the most used but it does not represent always the correct TBL characteristics. Therefore, the simplified load models of the present work could be inaccurate if compared to experimental data or to results derived from different TBL load models.

Finally, the simplified load models are applied to a well-known scaling procedure finalized to a further reduction of the computational cost. These results are extremely promising for the evaluation of the response of complex structural domains where, in principle, a large number of grid points and modal eigenvectors are required.

REFERENCES

[1] Corcos, G.M., 1963. Resolution of pressure in turbulence. Journal of Acoustical Society of America, 35, 192-199.

[2] Willmarth, W.W., Wooldridge, C.E., 1962. Measurements of the fluctuating pressure at the wall beneath a thick turbulent boundary layer. Journal of Fluid Mechanics 14, 187-210.

[3] Blake, W.K., 1986. Mechanics of Flow Induced Sound and Vibration. Academic Press, Orlando.

[4] Bull, K.M., 1967. Wall pressure fluctuations associated with subsonic turbulent boundary layer flow. Journal of Fluid Mechanics 28, 719-754.

[5] Farabee, T.M., Casarella, M.J., 1991. Spectral features of wall pressure fluctuations beneath turbulent boundary layers. Physics of Fluids A 3, 2410-2420.

[6] Efimtsov, B.M., 1982. Characteristics of the field of turbulent wall pressure fluctuations at large Reynolds numbers. Soviet Phisics-Acoustics, 28(4),289-292.

[7] Ffowcs Williams, J.E., 1982. Boundary layer pressures and the Corcos model: a development to incorporate low wavenumber constraints. Journal of Fluid Mechanics 125, 9-25.

[8] Chase, D.M., 1980. Modelling the wavevector-frequency spectrum of turbulent boundary layer wall pressure. Journal of sound and Vibration 70 (1), 29-67.

[9] Smol'yakov, A.V., Tkachenko, V.M., 1991. Model of pseudonic turbulent wall pressures and experimental data. Soviet Physics-Acoustic 37(6), 627-631.

[10] Birgersson F., Ferguson N. S., Finnveden S., 2003. Application of the spectral finite element method to turbulent boundary layer induced vibration of plates. Journal of Sound and Vibration, 259, 873-891.

[11] Mazzoni D., 2003. An efficient approximation for the vibro-acoustic response of a turbulent boundary layer excited panel. Journal of Sound and Vibration, 264, 951-971.

[12] Maury C., Gardonio P., Elliott S.J., 2002. A wavenumber approach to modelling the response of a randomly excited panel, Part II: Application to aircraft panels excited by a turbulent boundary layer. Journal of Sound and Vibration, 252, 115-139.

[13] Hambric, S.A., Hwang, Y.F., Bonness W.K., 2004. Vibrations of plates with clamped and free edges excited by low-speed turbulent boundary layer flow. Journal of Fluids and Structures, 19, 93–110.

[14] Finnveden S., Birgersson, Ross U., Kremer T., 2005. A model of wall pressure correlation for prediction of turbulence-induced vibration. Journal of Fluids and Structures, 20, 1127-1143

[15] De Rosa S., Franco F., 2008. "Exact and numerical responses of a plate under a turbulent boundary layer excitation". Journal of Fluids and Structures, Vol.24, 212-230.

[16] Ichchou M. N., Hiverniau B., Troclet B., 2009. "Equivalent 'rain on the roof ' loads for random spatially correlated excitations in the mid frequency range". Journal of Sound and Vibration, Vol.322, pp. 926-940.

[17] Ciappi E., Magionesi F., De Rosa S., Franco F., 2009. "Hydrodynamic and hydroelastic analyses of a plate excited by the turbulent boundary layer". Journal of Fluids and Structures, Vol. 25, 321-342.

[18] Hong C., Shin K.K., 2010. "Modelling of wall pressure fluctuations for finite element structural analysis". Journal of Sound and Vibration, Vol. 329, 1673-1685.

[19] Elishakoff I., 1983. Probabilistic Methods in the Theory of Structures. John Wiley & Sons, New York.

[20] De Rosa S., Pezzullo, G.,Lecce, L., Marulo, F., 1994. Structural Acoustic Calculations in the Low Frequency Range. AIAA Journal of Aircraft, Vol.31(6), 1387-1394.

[21] De Rosa S., Franco F., 2008. "A scaling procedure for the response of an isolated system with high modal overlap factor". Mechanical Systems and Signal Processing, Vol.22, 1549-1565.

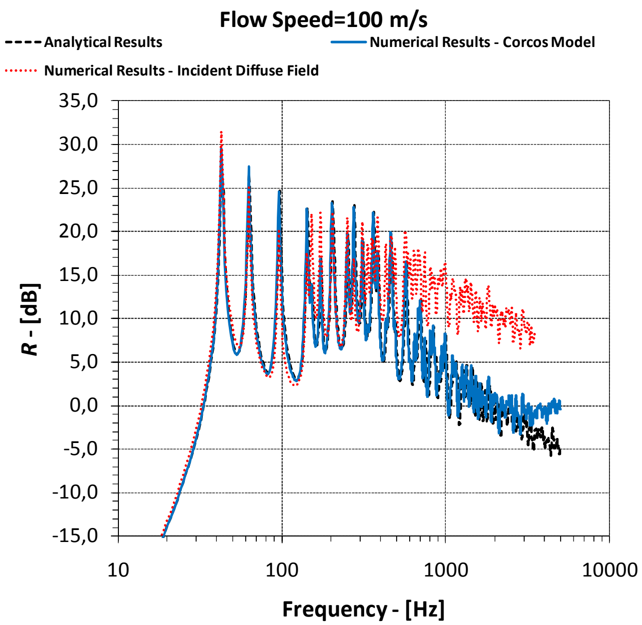

FIGURE 8: THE EFFECT OF DIFFERENT COHERENCE FUNCTIONS.

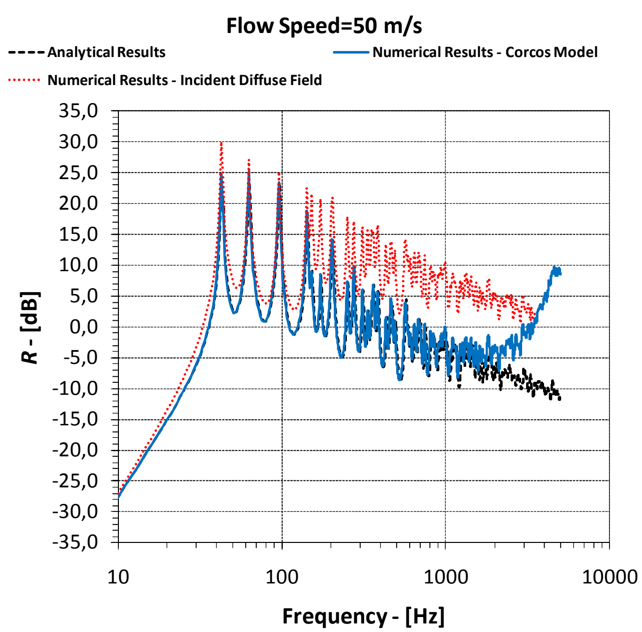

FIGURE 9: THE EFFECT OF DIFFERENT COHERENCE FUNCTIONS.

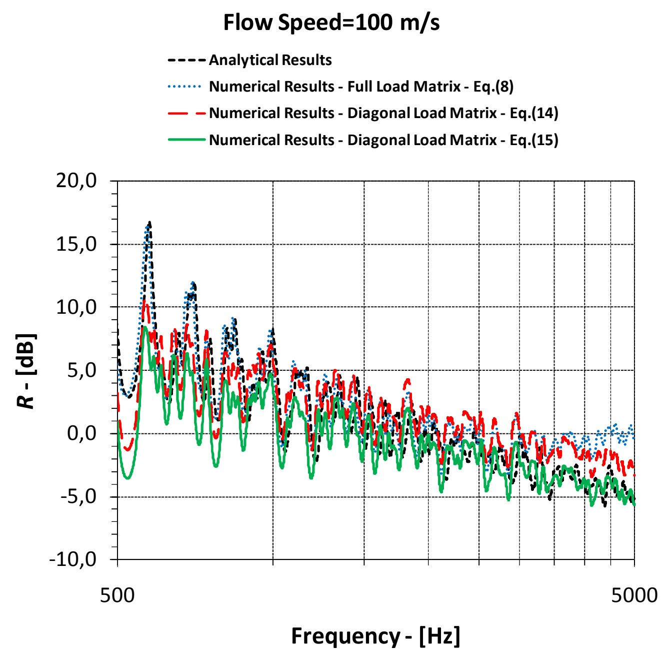

FIGURE 10: COMPARISON AMONG NUMERICAL RESULTS WITH DIFFERENT S_{FF} MATRICES.

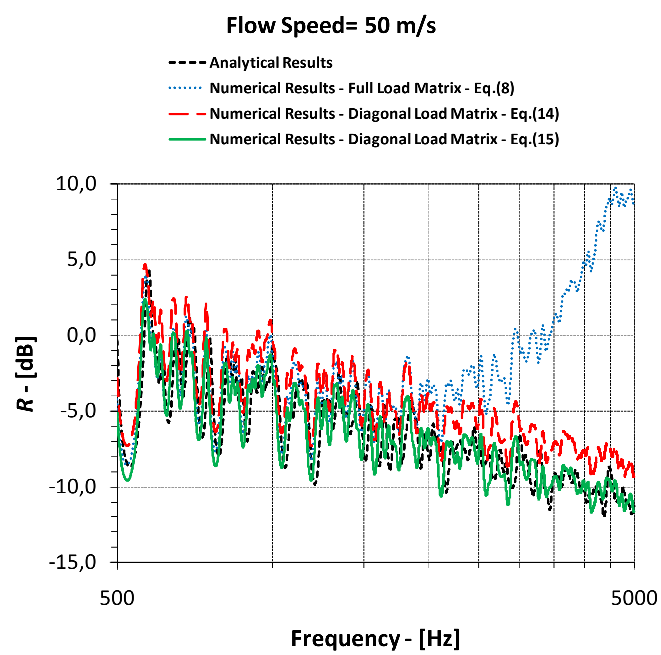

FIGURE 11: COMPARISON AMONG NUMERICAL RESULTS WITH DIFFERENT S_{FF} MATRICES.

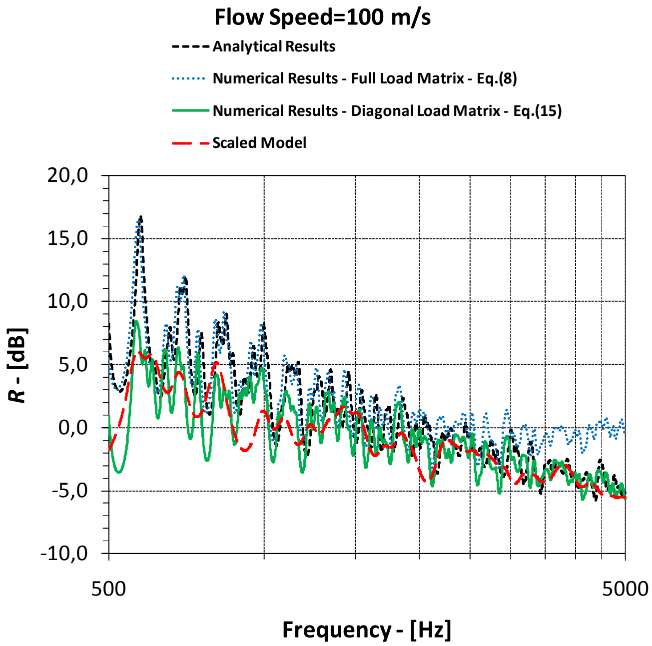

FIGURE 12: THE SCALED STRUCTURAL MODEL VS. ORIGINAL ONES.

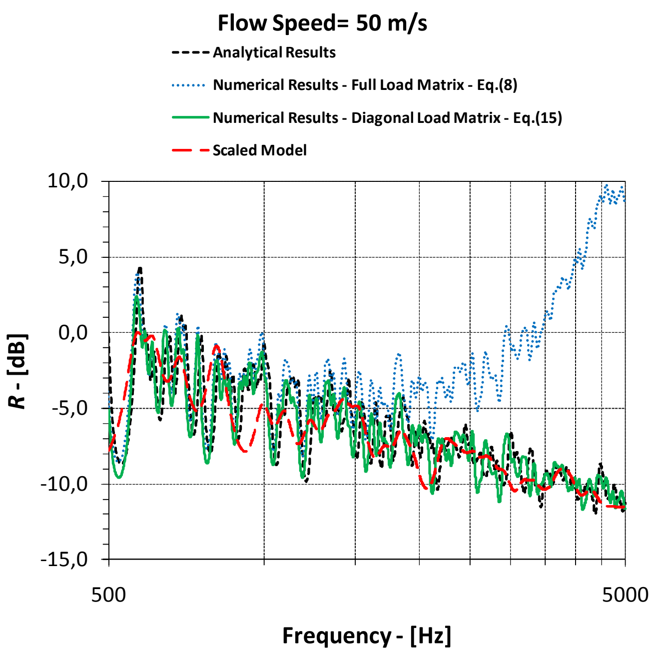

FIGURE 13: THE SCALED STRUCTURAL MODEL VS. ORIGINAL ONES.